

Thermodynamic and kinetic investigations in a solar thermochemical energy storage system with the combined steam and dry methane reforming

Fan Jiao^{1,2,3}, Buchu Lu^{2,3}, Chen Chen^{2,3,4}, Qibin Liu^{2,3*}

1 School of Energy, Power and Mechanical Engineering, North China Electric Power University, Beijing, 102206, China

2 Institute of Engineering Thermophysics, Chinese Academy of Sciences, Beijing, 100190, China

3 University of Chinese Academy of Sciences, Beijing, 100190, China

4 Zhejiang University of Technology, Hangzhou, Zhejiang, 310032, China

ABSTRACT

To make efficient use of natural gas resource and realize carbon-free emission, a solar thermochemical energy storage system with the combined steam and dry methane reforming is proposed in this study. In the system, the methane reforming reaction is driven by concentrated solar energy, which upgrades solar thermal energy into chemical energy in the form of the syngas products. A reactor model that considers multiple reactions system and kinetic rate equations is used for the performance simulation of the thermochemical energy storage system. The results show that the distributions of temperature, mole fraction of components and conversion along reactor axis direction are uneven. The steam methane reforming reaction mainly consumes CH₄ at the front part of the reactor, and the dry methane reforming reaction dominates the reaction system at the latter part of the reactor. The highest thermochemical energy storage efficiency can reach 61% under the condition of the stoichiometric feed ratio and 1 bar. The research findings provides an efficient and stable method for the reduction of natural gas consumption and the utilization of solar energy

Keywords: Combined steam and dry reforming; Solar energy; Thermochemical energy storage; Kinetic model; Thermodynamics

NONMENCLATURE

Abbreviations

CSDMR	Combined steam and dry methane reforming
DMR	Dry methane reforming
DNI	Direct normal irradiation

SMR	Steam methane reforming
<i>Symbols</i>	
A	Area
c_p	Specific heat
f	Mole flow rate
k	Rate constant
p	Pressure
r	Reaction rate
T	Temperature
ΔG_m^\ominus	Standard Gibbs free energy change
ΔS_m^\ominus	Standard entropy change
x	Axial coordinate
ρ	Catalytic bed density

1. INTRODUCTION

Nowadays, fossil fuels provide more than 80% of energy for human beings production and life [1]. Excessive carbon emission from the combustion of fossil fuels results in severe energy and environmental issues. In order to alleviate global warming, hydrogen has been regarded to be the alternative substitute due to its high energy density and carbon-free combustion. Hydrogen production through renewable energy is considered to be one of the ultimate technology routes for future.

Among the hydrogen production methods, methane steam reforming (SMR) contributes to the majority of world's hydrogen production due to the lower cost (less than 2\$/kg_{H2}) [2]. Combustion of part of the feed gas (natural gas) for driving the SMR causes high global warming potential. The solar driven SMR which converts solar thermal energy into hydrogen chemical energy has attracted increasing attentions due to the fuel saving and the reduction of carbon emission. However, the high H₂/CO ratio makes SMR difficult to be directly applied to the Fischer-Tropsch synthesis.

Selection and peer-review under responsibility of the scientific committee of the 12th Int. Conf. on Applied Energy (ICAE2020).

Copyright © 2020 ICAE

Methane reforming with CO₂ (dry methane reforming, DMR) has an H₂/CO ratio of 1 in syngas products, which is ideally applied to the Fischer-Tropsch synthesis. In addition, DMR produces syngas from two greenhouse gases (CH₄ and CO₂). However, this process is not commercially competitive, because the serious carbon deposition in catalysis limits its stability for long-time operation.

Combined steam and dry methane reforming (CSDMR) not only acquires desired H₂/CO ratio, but mitigates the carbon deposition effect due to the vapor-rich environment. Gangadharan et al. [3] believed that the CSDMR process has a lower carbon footprint as compared with SMR through an environmental evaluation. Jang et al. [4] conducted a thermodynamic equilibrium analysis for CSDMR with total Gibbs free energy minimization methods. They found that H₂/CO ratio can be controlled by changing CO₂/H₂O ratio, and coke formation can be avoided when (CO₂+H₂O)/CH₄ ratio is larger than 1.2. Soria et al. [5] experimentally studied CSDMR on Ru/ZrO₂-La₂O₃ at low temperature, and concluded that the combined process could help improve CH₄ conversion based on the Gibbs free energy minimization method.

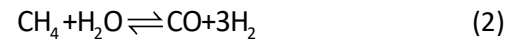
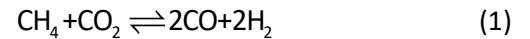
Previous studies on CSDMR focus mainly on chemical level. The performance and potential of a solar driven CSDMR system are not studied in detail. The characteristics of CSDMR in a solar reactor need to be investigated. In addition, previous studies for CSDMR are based on the Gibbs free energy minimization method. However, the species can hardly reach chemical equilibrium in a solar reactor due to the limited reactor size and large flow rate.

Hence, a solar thermochemical energy storage system with CSDMR is proposed and analyzed in this paper. To consider the real non-equilibrium process in a solar reactor, a kinetic model of CSDMR is established to analyze the thermochemical properties of the solar reactor. The main contributions of this study can be summarized as follows:

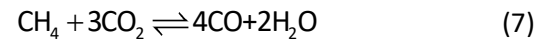
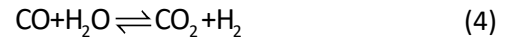
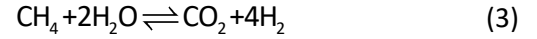
- 1) A solar thermochemical energy storage system with CSDMR is proposed;
- 2) The temperature, mole fraction and conversion distributions are obtained by simulating the non-equilibrium process with kinetic model.
- 3) Parameter studies are conducted for a high conversion efficiency.

2. MULTIPLE REACTIONS SYSTEM IN THE COMBINED STEAM AND DRY METHANE REFORMING

The objective reactions of CSDMR system are:



However, several side reactions also occur simultaneously, including:



Reactions (1)-(4) are considered in CSDMR system in the following parts, according to the studies of Xu et al. [6] and Olsbye et al. [7].

3. MATHEMATICAL MODE

The process flow configuration of the solar thermochemical energy storage system of CDSRM is depicted in Fig (1), including the heliostat field, a solar reactor, a cooler, and a fuel cell. The solar reactor is designated to be a cylindrical packed bed reactor, in which the commercial sulfide nickel catalyst Ni-0309S supported on gamma alumina is used. Methane steam and dry reforming reactions take place in the solar reactor, converting reactants (CH₄, H₂O and CO₂) to syngas products (H₂ and CO) and upgrading solar thermal energy into the syngas chemical energy. The mixture from the reactor is cooled down to a low temperature (or surroundings temperature), and then enters the fuel cell for power, which is converted back to the reactants to form a material loop.

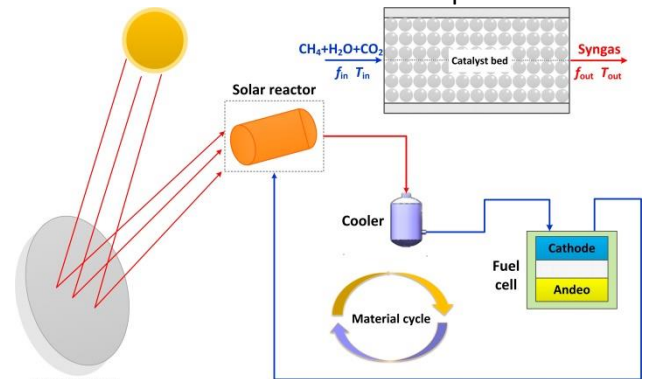


Fig (1) Process flow diagram of the solar thermochemical energy storage system

In terms of previous thermodynamic reactor model, most studies believed that all the reactions approach the chemical equilibrium, and the total Gibbs free energy of components at the outlet of reactor is minimized. The equilibrium state is only probably achieved under the condition of infinite reaction time

(or very long time). However, the reactions often cannot reach the chemical equilibrium due to the limit size of the reactor, large flow rate, etc. In fact, the kinetic characteristics of reactions determine the conversion of components, and further affect the energy behavior. Before stating the simulation study, some assumptions are made in order to use the pseudo-homogeneous model:

- 1) The system operates at a steady state;
- 2) This model does not consider the radial variation of concentrate and temperature;
- 3) Components in gaseous phase are considered as the ideal gas.

In the solar reactor, reactions (1)-(4) are used in the CSDMR simulation. The rate equations of the kinetic model can refer to Xu et al. [6] and Olsbye et al. [7].

$$r_1 = \frac{k_1 (P_{\text{CH}_4} P_{\text{CO}_2} - P_{\text{H}_2}^2 P_{\text{CO}}^2 / K_1)}{(1 + K_{\text{CH}_4} P_{\text{CH}_4} + K_{\text{CO}} P_{\text{CO}})(1 + K_{\text{CO}_2} P_{\text{CO}_2})} \quad (9)$$

$$r_2 = \frac{k_2}{P_{\text{H}_2}^{2.5}} \left[P_{\text{CH}_4} P_{\text{H}_2\text{O}} - \frac{P_{\text{H}_2}^3 P_{\text{CO}}}{K_2} \right] / \text{DEN}^2 \quad (10)$$

$$r_3 = \frac{k_3}{P_{\text{H}_2}^{3.5}} \left[P_{\text{CH}_4} P_{\text{H}_2\text{O}}^2 - \frac{P_{\text{H}_2}^4 P_{\text{CO}_2}}{K_3} \right] / \text{DEN}^2 \quad (11)$$

$$r_4 = \frac{k_4}{P_{\text{H}_2}} \left[P_{\text{CO}} P_{\text{H}_2\text{O}} - \frac{P_{\text{H}_2} P_{\text{CO}_2}}{K_4} \right] / \text{DEN}^2 \quad (12)$$

$$\text{DEN} = 1 + K_{\text{CO}} P_{\text{CO}} + K_{\text{H}_2} P_{\text{H}_2} + K_{\text{CH}_4} P_{\text{CH}_4} + \frac{K_{\text{H}_2\text{O}} P_{\text{H}_2\text{O}}}{P_{\text{H}_2}} \quad (13)$$

where r_i is the rate of reaction i ($i=1-4$); k_i is the kinetic rate constant of reaction i ; K_i represents the equilibrium constant of reaction i ; P_j refers to the partial pressure of gas species ($j=\text{CH}_4, \text{H}_2\text{O}, \text{CO}_2, \text{CO}$ and H_2); K_j is the adsorption constant of species j . Relevant kinetic parameters are demonstrated in Table 1 [8, 9].

Material balance equations in the solar reactor are determined by:

$$\frac{df_{\text{CH}_4}}{dx} = A \rho_b \cdot (-r_1 - r_2 - r_3) \quad (14)$$

$$\frac{df_{\text{H}_2\text{O}}}{dx} = A \rho_b \cdot (-r_2 - 2r_3 - r_4) \quad (15)$$

Table 1 Kinetic parameters for reaction (1)-(4) [8, 9]

	Parameter	Unit	Value
Kinetic rate constants	k_1	mol/(kg _{cat} ·s·bar ²)	$8.08 \times 10^2 \exp \left[\frac{-234851}{R_m} \left(\frac{1}{T} - \frac{1}{T_{\text{ref}}} \right) \right]$
	k_2	mol·bar ^{0.5} /(kgcat·s)	$9.408 \times 10^{11} \exp[-209500/(R_m T)]$
	k_3	mol·bar ^{0.5} /(kgcat·s)	$2.14 \times 10^9 \exp[-211500/(R_m T)]$
	k_4	mol/(kgcat·s·bar)	$5.43 \times 10^5 \exp[-70200/(R_m T)]$
Equilibrium constants	K_1	bar ²	$4.45 \times 10^9 \exp \left[\frac{-160940}{R_m} \left(\frac{1}{T} - \frac{1}{T_{\text{ref}}} \right) \right]$
	K_2	bar ²	$5.75 \times 10^{12} \exp(-11500/T)$
	K_3	bar ²	$7.24 \times 10^{10} \exp(-21600/T)$
	K_4	-	$1.26 \times 10^{-2} \exp(4600/T)$
Adsorption constants	K_{CH_4}	bar ⁻¹	$1.995 \times 10^{-3} \exp(36650/T)$
	$K_{\text{H}_2\text{O}}$	bar ⁻¹	$1.68 \times 10^4 \exp[-85770/(R_m T)]$
	K_{CO_2}	bar ⁻¹	$5.97 \times 10^{-2} \exp[52670/(R_m T)]$
	K_{H_2}	bar ⁻¹	$7.05 \times 10^{-9} \exp[82550/(R_m T)]$
	K_{CO}	bar ⁻¹	$8.11 \times 10^{-5} \exp[70230/(R_m T)]$

[§] $T_{\text{ref}}=1123.15\text{K}$

$$\frac{df_{\text{CO}_2}}{dx} = A\rho_b \cdot (-r_1 + r_3 + r_4) \quad (16)$$

$$\frac{df_{\text{CO}}}{dx} = A\rho_b \cdot (2r_1 + r_2 - r_4) \quad (17)$$

$$\frac{df_{\text{H}_2}}{dx} = A\rho_b \cdot (2r_1 + 3r_2 + 4r_3 + r_4) \quad (18)$$

where A is the cross sectional area of the reactor; ρ_b represents the density of the catalytic bed; f_j refers to the molar flow rate of the component j ; x is the axial coordinate along the reactor.

The variation of the component concentration causes the energy change. The energy conservation equation can be written as:

$$\sum_j f_j c_{p,j} \frac{dT}{dx} = \rho_b A \sum_{i=1}^4 r_i (-\Delta H_i) + A Q_{\text{solar}} - A Q_{\text{loss}} \quad (19)$$

where T is the temperature of the gaseous components; ΔH_i is the enthalpy change of the reactions; $c_{p,j}$ refers to the specific heat of species j ; Q_{solar} is the heat from absorbing solar radiation energy, and Q_{loss} is the radiation loss. Q_{solar} can be calculated by:

$$Q_{\text{solar}} = \alpha q_0 \exp(-\alpha s) \quad (20)$$

where α is the absorption coefficient of the catalytic bed for solar radiation; s is the penetrated length of solar radiation; q_0 is solar energy flux density, which can be computed by:

$$q_0 = DNI \cdot A_a \cdot \eta_{\text{op}} \quad (21)$$

where DNI is the direct normal irradiation; A_a represents the effective area of the heliostat field; η_{op} refers to the optical efficiency of the heliostat field. Q_{loss} can be written as:

$$Q_{\text{loss}} = 4\varepsilon\sigma_B (T^4 - T_0^4) \quad (22)$$

where ε is radiation loss coefficient and σ_B is the Stefan-Boltzmann constant.

At the inlet of the solar reactor, the boundary temperature and molar flow rate are:

$$f_j|_{x=0} = f_j^0 \quad (23)$$

$$T|_{x=0} = T_0 \quad (24)$$

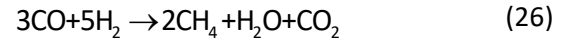
where f_j^0 is the inlet feed rate of component j and T_0 is the surroundings temperature.

Utilizing the boundary conditions to solve the material balance and energy conservation equations, the concentration and temperature of the components at the outlet of the solar reactor are acquired.

The outlet mixture of the solar reactor enters to the cooler, which is cooled from high temperature to T_0 . The heat rejected to the surroundings is calculated by:

$$Q_{\text{cooler}} = \sum_j f_j H_{j,T_{\text{out}}} - \sum_j f_j H_{j,T_0} \quad (25)$$

In order to make a closed-loop, an ideal H_2/CO fuel cell is adopted for acquiring maximum work from syngas products. Assuming that the reaction taking place in the fuel cell is:



Thus, the theoretical power and released heat are determined by:

$$P_{\text{FC}} = -n_{\text{FC}} \Delta G_m^\ominus \Big|_{3\text{CO} + 5\text{H}_2 \rightarrow 2\text{CH}_4 + \text{H}_2\text{O} + \text{CO}_2 @ T_0} \quad (27)$$

$$Q_{\text{FC}} = -n_{\text{FC}} T_0 \Delta S_m^\ominus \Big|_{3\text{CO} + 5\text{H}_2 \rightarrow 2\text{CH}_4 + \text{H}_2\text{O} + \text{CO}_2 @ T_0} \quad (28)$$

To evaluate the performance of the solar reactor and the thermochemical energy storage system, two criteria are used, i.e., conversion rate and cycle efficiency.

$$X_{\text{CH}_4} = \frac{f_{\text{CH}_4}^0 - f_{\text{CH}_4}^{\text{out}}}{f_{\text{CH}_4}^0} \times 100\% \quad (29)$$

$$X_{\text{H}_2\text{O}} = \frac{f_{\text{H}_2\text{O}}^0 - f_{\text{H}_2\text{O}}^{\text{out}}}{f_{\text{H}_2\text{O}}^0} \times 100\% \quad (30)$$

$$X_{\text{CO}_2} = \frac{f_{\text{CO}_2}^0 - f_{\text{CO}_2}^{\text{out}}}{f_{\text{CO}_2}^0} \times 100\% \quad (31)$$

$$\eta_{\text{cycle}} = \frac{P_{\text{FC}}}{DNI \cdot A_a} \quad (32)$$

Table 2 Baseline parameters for calculation

Parameters	Values
Area of heliostat field, A_a	800m ²
Reactor length, L	2m
Reactor diameter, D	1m
Catalytic bed density, ρ_b	1500kg/m ³
Penetrated length, s	0.05m
Radiation loss coefficient, ε	1
Optical efficiency, η_{op}	0.85 ^[10]

4. RESULTS AND DISCUSSION

The performance of the solar reactor and the overall thermochemical energy storage system are evaluated in this section. The feed gases at the inlet of the solar reactor consists of CH_4 , H_2O and CO_2 ($\text{CH}_4/\text{H}_2\text{O}/\text{CO}_2=2/1/1$) with the temperature of 298.15K. Other baseline parameters for the simulation are listed in Table 2. By solving the material balance and energy conservation equations, the distributions of temperature, mole fraction and conversion along the axial direction of catalytic bed are obtained, and the results are shown in Figs (2)-(4). The \bar{x} is introduced as the dimensionless reactor length, defined as $\bar{x} = x/L$.

From Fig (2), it can be known that the temperature of the fluid increases with the increasing of \bar{x} . The rising rate of temperature decreases (Curve slope reduces). This is because the large temperature difference between the reactor wall and components contributes a high heat transfer rate near the inlet of the reactor, the temperature of the working fluid is elevated rapidly. With the reduction of the temperature difference of heat transfer, the rate reduces. The outlet temperature of the solar reactor reaches 776K.

Fig (3) shows the mole fraction distribution in axial direction of the reactor. The marked change of mole fraction of components starts at around $\bar{x}=0.03$, indicating that the temperature meets the reaction requirement at current pressure. The mole fraction of CH_4 and H_2O reduces with the increasing \bar{x} . The tendency of mole fraction of CO_2 is influenced by reactions (1) and (3). The main reaction (1) is endothermic and takes places at a high temperature. The reaction (3), called water gas shifting reaction, is exothermic, which proceeds at a lower temperature. When the fluid enters the solar reactor, the reaction (3) dominates the variation of CO_2 mole fraction due to the low temperature. The temperature is increased along \bar{x} , restricting reaction (3). The main reaction (1) starts to dominate the change of mole fraction of CO_2 . In term of H_2 and CO , their mole fraction rises gradually along the dimensionless reactor length. The increase rate of H_2 mole fraction is larger than that of CO , because the water gas shifting reaction (reaction (3)) converts part of CO to H_2 .

The variations in the conversion of different components along \bar{x} are shown in Fig (4). The negative CO_2 conversion rate results from the yield of CO_2 by the reaction (3) larger than the CO_2 consumption in DMR at a low temperature, which is accordance with the variation trend of CO_2 mole fraction in Fig (3). With the increase of \bar{x} , H_2O is converted at a larger rate at the front part of the reactor, and this rate decreases gradually when approaching to the reactor outlet. CO_2 is consumed rapidly at the latter part of the reactor. This indicates that the steam reforming reaction (2) dominates the conversion of CH_4 near the reactor inlet, and dry reforming reaction mainly consumes CH_4 in the back half of the reactor. The conversions of CH_4 , H_2O and CO_2 at the outlet of reactor are 58.7%, 73.8% and 43.7%, respectively.

The reactant conversion can be raised with a higher reaction temperature by increasing the area of the heliostat field. Fig (5) shows the variation of

conversion and efficiency as a function of A_a . It can be known that the reactant conversions increase with the increasing of A_a . This is because the larger area of the heliostat field is, the higher reaction temperature can be reached, leading to more converted reactants. The highest efficiency under the simulation condition can reaches 61%. In addition, with the increase of A_a , the conversion of CO_2 increases rapidly, indicating that the dry reforming reaction is enhanced effectively.

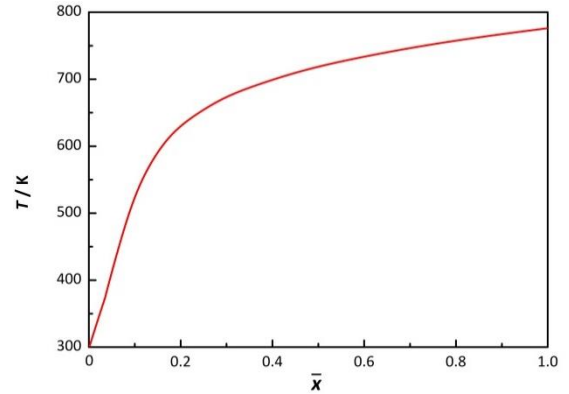


Fig (2) Variation of temperature along the dimensionless reactor length

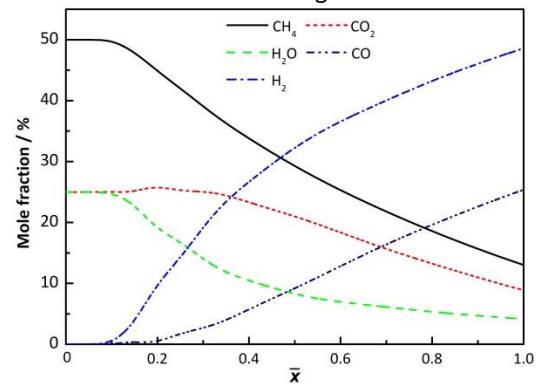


Fig (3) Variation of mole fraction of different components along the dimensionless reactor length

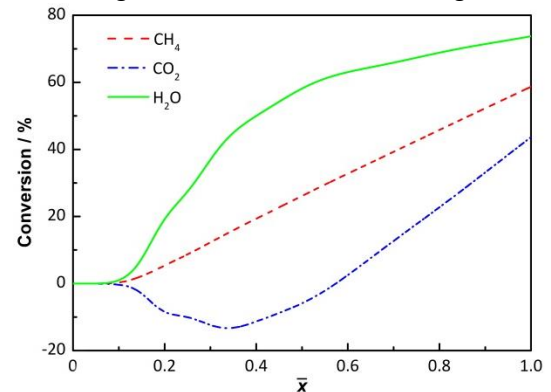


Fig (4) Variatiion of conversion of different reactants along the dimensionless reactor length

Fig. (6) shows the effect of the reaction pressure on conversion and cycle efficiency. The overall trend of conversion and thermochemical energy storage

efficiency reduces with the increase of the reaction pressure. This is because the objective reactions (1) and (2) as well as side reaction (3) are all the reactions, in which the mole number of products is larger than that of reactants. The high reaction pressure is not beneficial for the conversion of reactants. Also, the cycle efficiency is reduced.

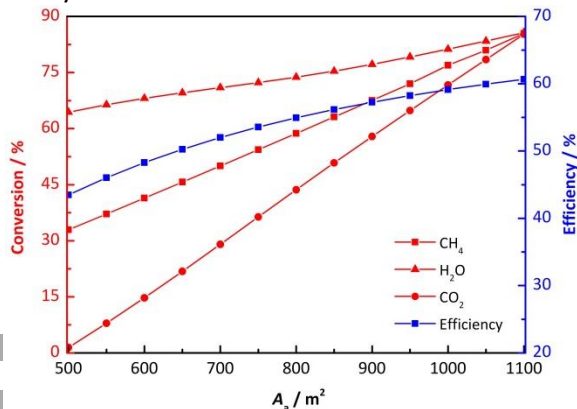


Fig (5) Variation of conversion and efficiency as a function of solar heliostat field area

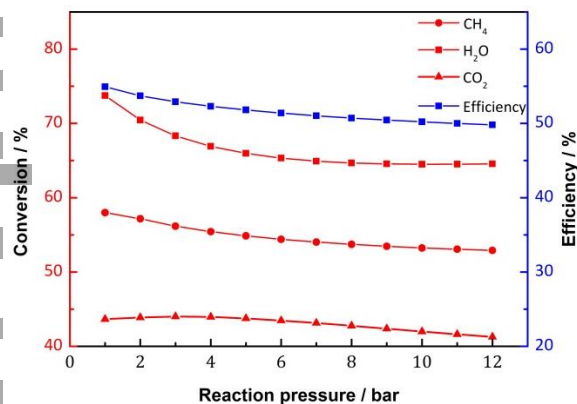


Fig (6) Effect of reaction pressure on conversion and efficiency

5. CONCLUSIONS

This paper conducts thermodynamic and kinetic studies in a solar thermochemical energy storage system with the combined steam and dry methane reforming. The main conclusions are summarized as follows.

- 1) The distributions of temperature, mole fraction and conversion along the axial direction of the solar reactor are uneven.
- 2) The conversion of CH₄ at the front part of the reactor is dominated by the steam reforming of methane; and the dry reforming of methane mainly consumes CH₄ at the latter part of the reactor.
- 3) Different heliostat field area greatly affects the conversion of components and efficiency. The highest thermochemical energy storage efficiency can reach 61% with the heliostat field area of

1100m² under the condition of the stoichiometric feed ratio (CH₄/H₂O/CO₂=2/1/1) and 1 bar.

ACKNOWLEDGEMENT

The authors appreciate the financial support provided by the Basic Science Center Program for Ordered Energy Conversion of the National Natural Science Foundation of China (No.51888103) and the National Natural Science Foundation of China (No. 51722606).

REFERENCE

- [1] BP. Statistical Review of world energy, 2020 | 69th Edition. In Bp.
- [2] Safari F, Dincer I. A review and comparative evaluation of thermochemical water splitting cycles for hydrogen production. *Energy Conv. Manag.* 2020; 205:112182.
- [3] Gangadharan P, Kanchi KC, Lou HH. Evaluation of the economic and environmental impact of combining dry reforming with steam reforming of methane. *Chem. Eng. Res. Des.* 2012; 90:1956-68.
- [4] Jang WJ, Jeong DW, Shim JO, Kim HM, Roh HS, Son IH, Lee SJ. Combined steam and carbon dioxide reforming of methane and side reactions: Thermodynamic equilibrium analysis and experimental application. *Appl. Energy.* 2016; 173:80-91.
- [5] Soria MA, Mateos-Pedrero C, Guerrero-Ruiz A, Rodriguez-Ramos I. Thermodynamic and experimental study of combined dry and steam reforming of methane on Ru/ ZrO₂-La₂O₃ catalyst at low temperature. *Int. J. Hydrog. Energy.* 2011; 36: 15212-20.
- [6] Xu JG, Froment GF. Methane steam reforming, methanation and water-gas shift: 1. Intrinsic kinetics. *AIChE J.* 1989; 35:88-96.
- [7] Olsbye U, Wurzel T, Mleczko L. Kinetic and reaction engineering studies of dry reforming of methane over a Ni/La/Al₂O₃ catalyst. *Ind. Eng. Chem. Res.* 1997; 36:5180-8.
- [8] Hoang DL, Chan SH, Ding OL. Kinetic and modelling study of methane steam reforming over sulfide nickel catalyst on a gamma alumina support. *Chem. Eng. J.* 2005; 112: 1-11.
- [9] Park N, Park MJ, Baek SC, Ha KS, Lee YJ, Kwak G, Park HG, Jun KW. Modeling and optimization of the mixed reforming of methane: Maximizing CO₂ utilization for non-equilibrated reaction. *Fuel.* 2014; 115:357-65.
- [10] Su BS, Han W, Jin HG. Proposal and assessment of a novel integrated CCHP system with biogas steam reforming using solar energy. *Appl. Energy.* 2017; 206:1-11